Title

P16INK4a Upregulation Mediated by SIX6 Defines Retinal Ganglion Cell Pathogenesis in Glaucoma

Journal

Molecular Cell, 59(6)

ISSN

1097-2765

Authors

Skowronska-Krawczyk, D
Zhao, L
Zhu, J
et al.

Publication Date

2015-09-17

DOI

10.1016/j.molcel.2015.07.027

Peer reviewed

Article

Molecular Cell

P16INK4a Upregulation Mediated by *SIX6* Defines Retinal Ganglion Cell Pathogenesis in Glaucoma

Graphical Abstract

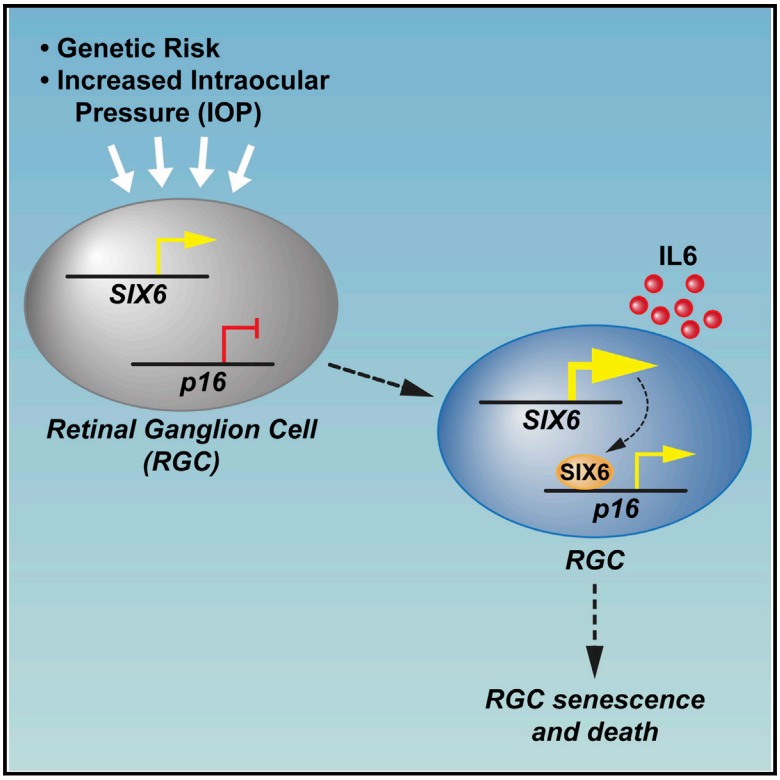

Highlights

- *SIX6* and *p16INK4a* contribute to POAG genetic risk synergistically
- SIX6 directly regulates *p16INK4a* expression
- *SIX6* and *p16INK4a* promote retinal ganglion cell senescence and death

Authors

Dorota Skowronska-Krawczyk, Ling Zhao, Jie Zhu, ..., Michael G. Rosenfeld, Yizhi Liu, Kang Zhang

Correspondence

yzliu62@yahoo.com (Y.L.), kang.zhang@gmail.com (K.Z.)

In Brief

Zhang et al. report *p16INK4a* as a downstream integrator of diverse signals, such as inherited genetic risk, age, and intraocular pressure, in the pathogenesis of glaucoma. They demonstrate that upregulation of *SIX6* upon stress directly increases *p16INK4a*, leading to retinal ganglion cell senescence and death.

Skowronska-Krawczyk et al., 2015, Molecular Cell *59*, 931–940
September 17, 2015
http://dx.doi.org/10.1016/j.molcel.2015.07.027

CellPress

Molecular Cell
Article

P16INK4a Upregulation Mediated by *SIX6* Defines Retinal Ganglion Cell Pathogenesis in Glaucoma

Dorota Skowronska-Krawczyk,[1,12] Ling Zhao,[1,2,12,13] Jie Zhu,[1,3] Robert N. Weinreb,[1] Guiqun Cao,[4] Jing Luo,[1] Ken Flagg,[1] Sherrina Patel,[1] Cindy Wen,[1] Martin Krupa,[1] Hongrong Luo,[1] Hong Ouyang,[1,2] Danni Lin,[1] Wenqiu Wang,[1,5] Gen Li,[4] Yanxin Xu,[4] Oulan Li,[4,6] Christopher Chung,[1] Emily Yeh,[1] Maryam Jafari,[1] Michael Ai,[1] Zheng Zhong,[2] William Shi,[1] Lianghong Zheng,[6] Michal Krawczyk,[1] Daniel Chen,[1] Catherine Shi,[1] Carolyn Zin,[1] Jin Zhu,[1] Pamela L. Mellon,[7] Weiwei Gao,[8] Ruben Abagyan,[1] Liangfang Zhang,[8] Xiaodong Sun,[5] Sheng Zhong,[9] Yehong Zhuo,[2] Michael G. Rosenfeld,[10] Yizhi Liu,[2,*] and Kang Zhang[1,2,4,9,11,*]

[1]Shiley Eye Institute, Department of Ophthalmology and Institute of Engineering in Medicine, University of California, San Diego, La Jolla, CA 92093, USA
[2]State Key Laboratory of Ophthalmology, Zhongshan Ophthalmic Center, Sun Yat-sen University, Guangzhou 510060, China
[3]Department of Ophthalmology, Xijing Hospital, Fourth Military Medical University, Xi'an 710032, China
[4]Molecular Medicine Research Center, State Key Laboratory of Biotherapy, West China Hospital, Sichuan University, Sichuan 610041, China
[5]Department of Ophthalmology, Shanghai First People's Hospital, School of Medicine, Shanghai JiaoTong University, Shanghai 20080, China
[6]Guangzhou KangRui Biological Pharmaceutical Technology Company Ltd., Guangzhou 510005, China
[7]Department of Reproductive Medicine
[8]Department of Nanoengineering
[9]Institute for Genomic Medicine
[10]Howard Hughes Medical Institute, School of Medicine
University of California, San Diego, La Jolla, CA 92093, USA
[11]Veterans Administration Healthcare System, San Diego, CA 92093, USA
[12]Co-first author
[13]Present address: Institute of Molecular Medicine, Peking University, Beijing 100871, China
*Correspondence: yzliu62@yahoo.com (Y.L.), kang.zhang@gmail.com (K.Z.)
http://dx.doi.org/10.1016/j.molcel.2015.07.027

SUMMARY

Glaucoma, a blinding neurodegenerative disease, whose risk factors include elevated intraocular pressure (IOP), age, and genetics, is characterized by accelerated and progressive retinal ganglion cell (RGC) death. Despite decades of research, the mechanism of RGC death in glaucoma is still unknown. Here, we demonstrate that the genetic effect of the *SIX6* risk variant (rs33912345, His141Asn) is enhanced by another major POAG risk gene, *p16INK4a* (cyclin-dependent kinase inhibitor 2A, isoform INK4a). We further show that the upregulation of homozygous *SIX6* risk alleles (CC) leads to an increase in *p16INK4a* expression, with subsequent cellular senescence, as evidenced in a mouse model of elevated IOP and in human POAG eyes. Our data indicate that *SIX6* and/or IOP promotes POAG by directly increasing *p16INK4a* expression, leading to RGC senescence in adult human retinas. Our study provides important insights linking genetic susceptibility to the underlying mechanism of RGC death and provides a unified theory of glaucoma pathogenesis.

INTRODUCTION

Primary open-angle glaucoma (POAG) is a group of progressive optic neuropathies characterized by a slow and progressive degeneration of retinal ganglion cells (RGCs) and their axons, resulting in a distinct appearance of the optic disc and a concomitant pattern of vision loss (Zhang et al., 2012). POAG is the most frequent type of glaucoma in the Western world, one of the world's leading causes of blindness, and the leading cause of blindness among African Americans (Weinreb et al., 2014). Intraocular pressure (IOP) and age are the leading risk factors for both the development and the progression of POAG.

Recent genome-wide association studies have indicated that the *SIX1-SIX6* and *p16INK4a* loci are among the strongest risk genes associated with POAG (Burdon et al., 2011; Osman et al., 2012; Wiggs et al., 2012). *SIX6* is a member of the homeodomain transcription factor family that has been shown to be required for proper eye development (Anderson et al., 2012). Although several common variants have been identified within this locus, the newly described SIX6 risk variant SIX6-rs33912345 (His141Asn) is strongly associated with POAG (Carnes et al., 2014; Iglesias et al., 2014; Osman et al., 2012), raising an intriguing question about the role of SIX6 in adult retina and in the pathology of POAG.

Expression of *p16INK4a* (cyclin-dependent kinase inhibitor 2A, isoform INK4a) is an indicator of irreversible growth arrest

A

Association of *SIX6* with POAG

SNP	Risk Allele	Case (n=1,130)	Control (n=4,036)	P Value (allelic)	OR (95% CI)
rs33912345	C	0.46	0.38	4.49E-12	1.39 (1.27-1.53)

B

Conservation of SIX6 His 141 across species

H/N

SIX6_*H.sapiens*	DGEQKTHCFKERTRHLLREWYLQDPYPNP
SIX6_*P.troglodytes*	DGEQKTHCFKERTRHLLREWYLQDPYPNP
SIX6_*M.mulatta*	DGEQKTHCFKERTRHLLREWYLQDPYPNP
SIX6_*C.lupus*	DGEQKTHCFKERTRHLLREWYLQDPYPNP
SIX6_*M.musculus*	DGEQKTHCFKERTRHLLREWYLQDPYPNP
SIX6_*R.norvegicus*	DGEQKTHCFKERTRHLLREWYLQDPYPNP
SIX6_*G.gallus*	DGEQKTHCFKERTRHLLREWYLQDPYPNP
SIX6_*D.rerio*	DGEQKTHCFKERTRHLLREWYLQDPYPNP

C

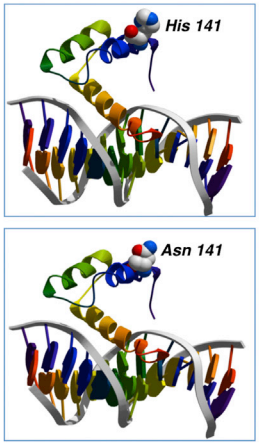

D

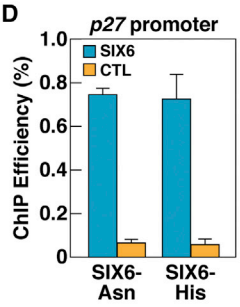

Figure 1. SIX6 Protein Residue 141 Variants Bind to DNA with Similar Efficiency

(A) Association of *SIX6* risk variant with POAG. Shown are the frequencies of SIX6 141 amino acid variants in the Caucasian population in correlation with POAG.

(B) Conservation of SIX6 His141 (risk) variant across the species; Asn141 (protective) variant is present only in human lineage.

(C) Computer modeling of SIX6 structure. Top: model of SIX6 with histidine at position 141; bottom: model of SIX6 with asparagine at position 141.

(D) ChIP-qPCR analysis of SIX6 binding to *p27* regulatory element in patient-derived lymphoblastoid cells shows similar efficiency of binding of both SIX6 variants. Experiments repeated three times, ±SD. CTL, negative control.

See also Figure S1.

(senescence) in cultured cells and tissues (Campisi, 2013; Krishnamurthy et al., 2004; Naylor et al., 2013). Senescent cells have been implicated in many age-associated degenerative phenotypes, often through secreted proteins, which are components of senescence-associated secretory phenotype (SASP) (Campisi, 2013). Interestingly, it has been reported that selective elimination of *p16Ink4a*-positive senescent cells can prevent or delay age-related deterioration of mouse tissue (Baker et al., 2011). *p16Ink4a* expression was found to be significantly elevated in a rat model of glaucoma (Burdon et al., 2011), suggesting a role for p16-dependent pathway in the progression of the disease.

Here, using a combination of genetic association and functional studies, we show that *SIX6* risk variant increases *p16INK4a* expression and leads to RGC senescence in cell culture, animal models, and human glaucoma retinas. This study provides insights into the mechanism of RGC death in glaucoma and suggests potential avenues for therapeutic intervention in glaucoma patients.

RESULTS

Association of *SIX6*-rs33912345 with Risk for POAG

We performed genetic association studies and identified one missense variant of *SIX6*, rs33912345 (Genbank: NM_007374.2, c.421C > A; Genbank: NP_031400.2, p.His141Asn), to be strongly associated with POAG. To further investigate the genetic association between *SIX6*-rs33912345 and POAG in the Caucasian population, rs33912345 (C/A) in the *SIX6* gene was genotyped using a single-nucleotide primer extension assay in 1,130 POAG patients and 4,036 controls. The C risk allele frequency of rs33912345 in *SIX6* was significantly higher in POAG patients (0.46) than in controls (0.38) (allelic $p = 4.49 \times 10^{-12}$, odds ratio [OR] 1.39, 95% CI 1.27–1.53) (Figure 1A). We proceeded to perform a replication study using a Mexican cohort with POAG and found a significant association ($p = 0.011$) (Table S1). We then performed meta-analysis using these two cohorts and another cohort reported in the literature (Carnes et al., 2014). Together, the combined results indicate a significant association (allelic $p = 4.84 \times 10^{-16}$) (Table S1).

The human risk allele His141 in *SIX6* is conserved across species (Figure 1B), and amino acid 141 is located in the homeodomain of the SIX6 protein. Three-dimensional modeling indicated that this residue is positioned outside of the DNA-binding surface and thus is predicted to have no impact on DNA binding (Figure 1C) but could rather influence the ability of SIX6 to interact with other transcription factors and co-factors. To assess both SIX6 variants in vivo for their efficiency of binding to DNA regulatory elements, we first tested the specificity of our SIX6 antibody by chromatin immunoprecipitation (ChIP) assay on chromatins isolated from wild-type (WT) and *Six6* knockout (KO) retinas. We observed that SIX6 protein could efficiently bind to the *p27* regulatory element (Figure S1A), previously reported to be directly recognized by *Six6* (Li et al., 2002). Using the same approach, we observed that both the His141 and Asn141 variants of the SIX6 protein can bind the *p27* regulatory element in patient-derived lymphoblastoid cells with similar efficiency (Figure 1D). Additionally, we overexpressed HA-tagged versions of SIX6 in HEK293T cells and tested their ability to bind to the *p27* regulatory element. ChIP experiments with antibodies specific to SIX6 protein or to the HA tag demonstrated that both forms of the SIX6 (His141 and Asn141) bind efficiently to the *p27* regulatory region (Figures S1B and S1C). We therefore concluded that the presence of neither variant of residue 141 alters SIX6 binding efficiency to this known DNA-regulatory element, confirming our protein modeling prediction.

Joint Effect of *SIX6* and *p16INK4a* on POAG Risk

Because *SIX6* and *p16INK4a* (Genbank: NM_000077) are the two genes showing the strongest genetic association with POAG risk, we investigated the joint effect of *SIX6*-rs33912345 and *p16INK4a*-rs3731239 on POAG risk using a logistic

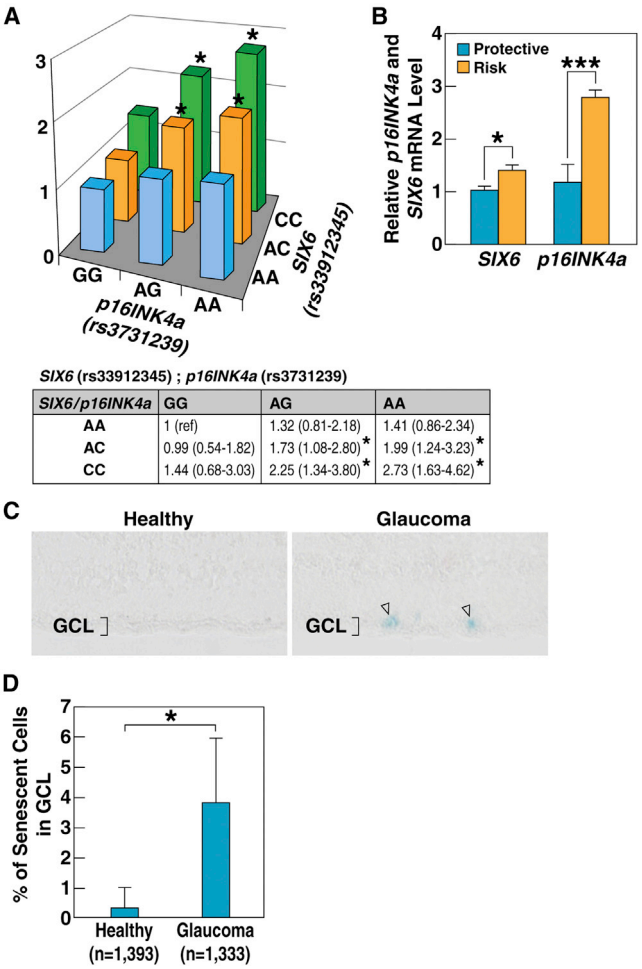

SIX6 (rs33912345) ; *p16INK4a* (rs3731239)

SIX6/*p16INK4a*	GG	AG	AA
AA	1 (ref)	1.32 (0.81-2.18)	1.41 (0.86-2.34)
AC	0.99 (0.54-1.82)	1.73 (1.08-2.80)*	1.99 (1.24-3.23)*
CC	1.44 (0.68-3.03)	2.25 (1.34-3.80)*	2.73 (1.63-4.62)*

Figure 2. Joint Effect of Specific Alleles of *SIX6* (rs33912345) and *p16INK4a* (rs3731239) Suggests Functional Interaction between the Two Genes

(A) Results of the logistic regression analysis, plotted as z axis by ORs.

(B) RT-qPCR analysis of mRNA expression of *SIX6* and *p16INK4a* in human lymphocytes stratified by their *SIX6* (rs33912345) genotypes. Four cell lines with rs33912345-AA (non-risk alleles) and four cell lines with rs33912345-CC (risk alleles) were analyzed. Relative mRNA levels were calculated by normalizing results with GAPDH and expressed relative to the AA genotype. The p values were calculated using two-tailed Student's t test (±SD; *$p < 0.05$, ***$p < 0.001$).

(C) SA-βgal staining of human retinas indicating larger numbers of senescent cells in retinas with POAG.

(D) Quantification of senescent cells in healthy and POAG retinas (*$p < 0.05$). See also Figure S2.

regression model and calculated ORs. A global two-locus (9′2) contingency table, enumerating all nine two-locus genotype combinations, was constructed. Compared with that of a baseline of non-risk alleles *SIX6*-rs33912345 AA and *p16INK4a*-rs3731239 GG, the OR of the risk alleles *SIX6*-rs33912345 CC and *p16INK4a*-rs3731239 AA was 2.73 ($p < 0.05$, 95% CI 1.63–4.62) (Figure 2A), suggesting their joint effect on POAG risk.

To investigate the correlation between *SIX6*-rs33912345 and *p16INK4*-rs3731239 genotypes and the expression of *SIX6* and *p16INK4a*, mRNA levels of both genes were measured in patient-derived human lymphoblastoid cells using reverse transcription followed by quantitative PCR (RT-qPCR). We detected higher *SIX6* levels (1.4-fold) in cell lines carrying the *SIX6* risk allele. In addition, the expression of *p16INK4a* mRNA was 2.3-fold higher in cells with risk genotype compared with the cells with protective genotype (Figure 2B). We further measured the levels of *p16INK4a* mRNA in retinas from healthy and glaucoma patients and observed significantly elevated expression in glaucoma eyes (Figure S2B). To investigate whether the elevated expression of *p16INK4a* correlated with increased cellular senescence, a senescence-associated β-galactosidase (SA-βgal) assay was performed on healthy and glaucoma human retinas. Consistently, retinas from glaucoma patients exhibited elevated senescence, as indicated by a significantly larger number of blue-positive cells in the ganglion cell layer (GCL) (Figures 2C, 2D, and S2A).

Transcriptional Regulation of *p16INK4a* by SIX6

To investigate whether SIX6 is involved in transcriptional regulation of *p16INK4a*, we transiently expressed SIX6-His141 or SIX6-Asn141 variants in human fetal retinal progenitor cells (fRPCs) and quantified *p16INK4a* mRNA levels using RT-qPCR. Significantly higher expression of *p16INK4a* mRNA was observed in SIX6-His141-transfected cells (Figure 3A). Similar trends were observed when SIX6-His141 and SIX6-Asn141 were expressed at similar levels in HEK293T cells (Figures 3B and 3C), which suggests that the effect of the variation in SIX6 is not cell type specific. To test whether both HA-tagged SIX6 protein variants can bind directly to *p16INK4a* promoter, we performed ChIP assays using anti-SIX6 and anti-HA antibodies. We observed that both protein variants bind to *p16INK4a* promoter with similar efficiency (Figure 3D and not shown). Taken together, these data suggest that SIX6 can act as a direct activator of *p16INK4a* gene and that the SIX6-His141 variant has more potential to activate *p16INK4a* expression.

Given that elevated expression of *p16INK4a* is a hallmark of cellular senescence (Campisi, 2013; Naylor et al., 2013), we tested whether transient overexpression of either variant of SIX6 (SIX6-His141 and SIX6-Asn141) could induce senescence in fRPCs. Interestingly, merely 24 hr post-transfection, fRPCs expressing SIX6-His141 variant underwent senescence twice as readily as those under control conditions or those transfected with SIX6-Asn141 variant, as assessed by a SA-βgal assay and by upregulation of interleukin-6 (IL6), a secretory marker of senescence (Figures 3E, 3F, and S3). Taken together, these data indicate that SIX6-His141 risk variant increased senescence in fRPCs by direct induction of *p16INK4a* expression.

Upregulation of *Six6* and *p16Ink4a* in a Mouse Model of Acute Glaucoma

Experimental ocular hypertension mouse models have been used extensively to study the relationship between IOP and the mechanism of glaucomatous optic neuropathy (Gross et al., 2003). To investigate the association of glaucoma in the context of *SIX6*-His risk variant and *p16INK4a* expression, we used a mouse glaucoma model in which the IOP is increased acutely. First, we analyzed the sequence of mouse *Six6* gene and noticed

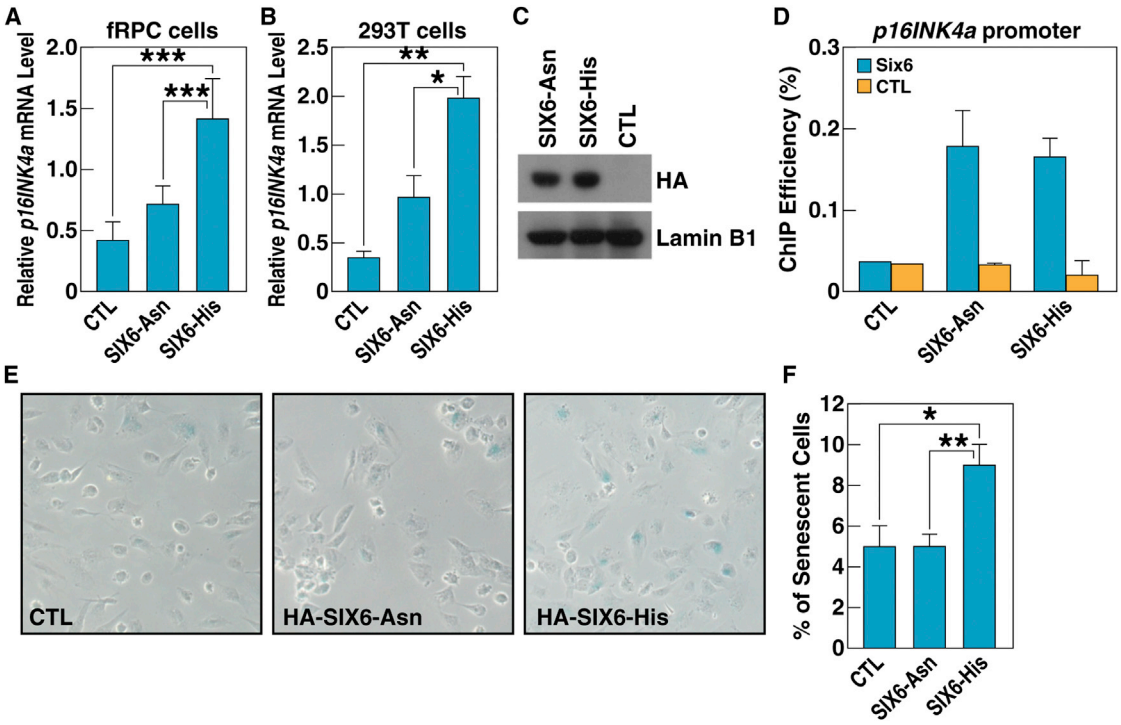

Figure 3. Increased Expression of *SIX6* Risk Variant Correlates with a Higher Senescence Rate

(A) RT-qPCR analysis shows that overexpression of *SIX6*-His variant increased *p16INK4a* expression in fRPCs. Experiments repeated three times; p values were calculated using two-tailed Student's t test (±SD; ***$p < 0.001$).

(B) RT-qPCR analysis shows that the overexpression of the *SIX6*-His variant increased *p16INK4a* expression in 293T cells. Experiments repeated three times; p values calculated using a two-tailed Student's t test (±SD; *$p < 0.05$, **$p < 0.01$).

(C) Western blot confirming similar levels of expression of both SIX6 variants in transient transfections experiments.

(D) ChIP-qPCR analysis of SIX6 variant association with *p16INK4a* promoter, showing similar level of binding.

(E) SA-βgal staining of the fRPCs transfected with either of the two *SIX6* variants showing higher ratio of senescence in cells transfected with SIX6-His141 risk variant.

(F) Quantification of β-galactosidase-positive cells in fRPCs transfected with *SIX6* variants. The p values were calculated using a two-tailed Student's t test (±SD; *$p < 0.05$, **$p < 0.01$).

See also Figure S3.

that mouse genome encodes only the *Six6*-His variant (Figure 1B). Western blot analysis confirmed that SIX6 was expressed in the adult retina at levels comparable with those observed in the embryonic stages (Figure 4A). When both *Six6* and *p16Ink4a* mRNA levels were measured 5 days after IOP elevation, both *Six6* and *p16Ink4a* mRNA expression levels were significantly higher in retinas from IOP-treated eyes compared with those from control eyes (Figure 4B). We also noted increased expression of *p15Cdkn2b* and *p19Arf* upon IOP elevation (Figures S4A and S4B).

Because SIX6 binds to *p16INK4a* promoter upon engineered expression in cell culture (Figure 3D), we asked if SIX6 could also bind to this promoter in adult mouse retina in vivo. To test this, we compared ChIP efficiency in chromatins isolated from WT and *Six6* KO retinas. We found that detectable signal could only be observed in WT retinas, not in $Six6^{-/-}$ retinas (Figure S4C). Further, we investigated whether SIX6 binding to *p16Ink4a* promoter in the retina was altered by IOP elevation. We performed a ChIP-qPCR assay in chromatins isolated from IOP-elevated and control retinas and observed that binding of SIX6 to the *p16Ink4a* promoter was significantly elevated upon increased IOP (Figure 4C). This phenomenon correlated with elevated recruitment of histone acetyltransferase p300, a known co-activator of *p16Ink4a* expression (Figure 4D) (Wang et al., 2008), and increased pan-acetylation of histone H3, a modification that is associated with active regulatory elements (Figure 4E) (Strahl and Allis, 2000). Importantly, there was no recruitment of SIX6 to *p19Arf* or *p15Cdkn2b* promoters upon IOP elevation (Figure S4D), suggesting that the effect of SIX6 on *p16Ink4a* is gene specific. We then used a SA-βgal assay to test if the cells in the treated retinas had undergone senescence. As expected, in five of five mice tested, we observed a dramatic accumulation of senescent cells in the IOP-treated retinas, compared with only a few senescent cells observed in untreated retinas (Figures 4F and S4E).

We further investigated whether it was the RGCs that underwent senescence in IOP-treated retinas. As expected, images of the retinal cross-sections showed that most of the senescent cells were localized in the GCL (Figure 5A). We performed immunohistochemistry using an anti-BRN3a antibody (an RGC marker) on IOP-treated and non-treated flat-mount retinas and

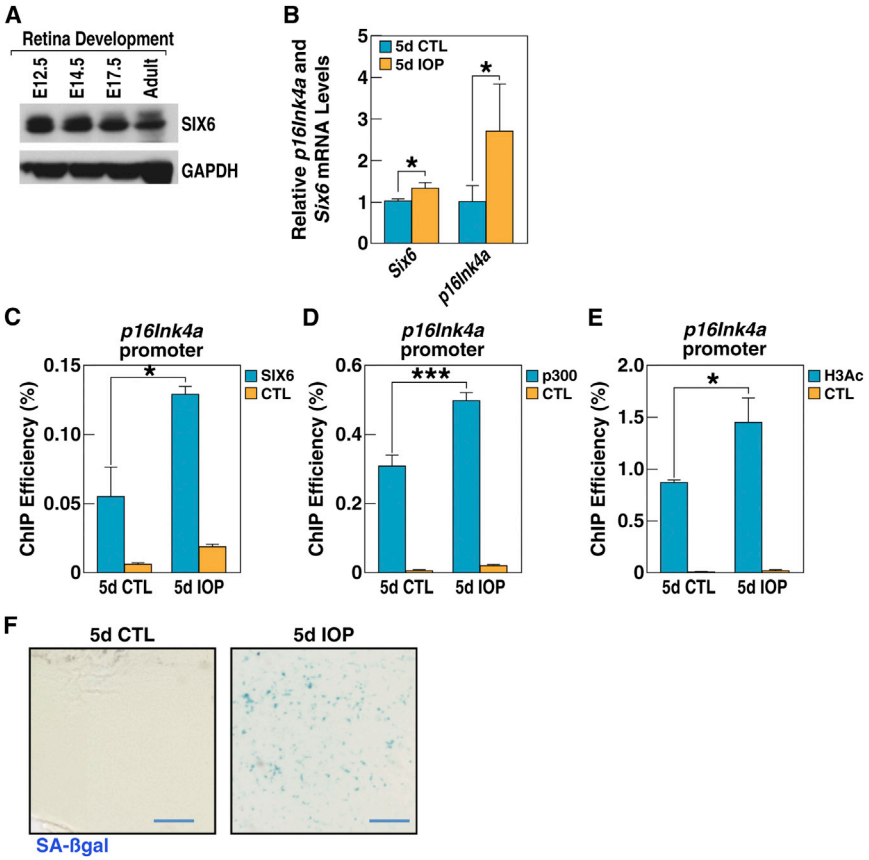

Figure 4. Increased Expression of *Six6* and Induction of Cell Senescence in Retinas upon IOP Elevation

(A) The expression of SIX6 protein in mouse retina during development and in the adult stage analyzed by western blotting.

(B) RT-qPCR analysis of *Six6* and *p16Ink4a* mRNA levels shows elevated expression of *Six6* and *p16Ink4a* in IOP-elevated mouse retinas 5 days after the induction of acute experimental glaucoma (5d IOP) compared with non-treated retina (5d CTL). Experiments were repeated in eight animals; p values calculated using a two-tailed Student's t test (±SD; *$p < 0.05$).

(C) ChIP-qPCR analysis of SIX6 protein binding shows its higher association with the *p16Ink4a* promoter in retinas subjected to acute IOP increase (5d IOP) compared with non-treated retina (5d CTL). Experiments repeated three times, p values calculated using a two-tailed Student's t test (±SD; *$p < 0.05$).

(D) ChIP-qPCR analysis shows higher levels of p300 association with *p16Ink4a* promoter upon experimental glaucoma (5d IOP) compared with non-treated retina (5d CTL). Experiments repeated three times; p values calculated using a two-tailed Student's t test (±SD; ***$p < 0.001$).

(E) ChIP-qPCR shows higher level of H3 acetylation at *p16Ink4a* promoter after acute IOP increase (5d IOP) compared with non-treated retina (5d CTL). Experiments repeated three times; p values were calculated using a two-tailed Student's t test (±SD; *$p < 0.05$).

(F) SA-βgal staining of flat-mount retinas isolated from treated and non-treated eyes. The large number of senescent cells is evident in IOP-treated tissue (blue bar, 100 μm).

See also Figure S4.

detected that most of the β-galactosidase-positive cells were also BRN3a positive (Figure 5B). We further confirmed these findings by comparing the β-gal staining pattern in Thy1-CFP transgenic mice, in which the RGCs are specifically marked by CFP fluorescence (Figures 5C and S5A) (Lindsey et al., 2013).

We next investigated the effects of engineered expression of SIX6 variants on the expression of *p16Ink4a* and SASP marker, IL6, in cultured RGCs. RGCs from rat retina were isolated by immunopanning using anti-Thy-1 antibody (Winzeler and Wang, 2013) (Figure 5D). The efficacy of this procedure was verified by cell morphology and Brn3a expression levels in isolated RGCs compared with whole retina cells (Figures S5D and S5E). Significantly, we observed increased expression of *p16Ink4a* and IL6 only in the RGCs in which we introduced the His variant of SIX6 (Figures 5E, S5F, and S5G). Consistently, there were remarkably more IL6-positive RGCs in the IOP-treated retinas than in controls (Figures S5B and S5C). Taken together, these data suggest that RGCs are the primary cells affected in this glaucoma model.

Lack of Either *Six6* or *p16Ink4a* Protects against RGC Death in Glaucoma

The homozygous *Six6* KO adult retinas display numerous abnormalities (Clark et al., 2013), especially in the RGC layer. Therefore, we decided to use heterozygous mice to test the role of SIX6 in induced senescence and in the regulation of *p16Ink4a* expression. As before, acute IOP elevation was applied, and retinas were collected and assayed 5 days after IOP. In contrast to the WT littermates, reduced *Six6* expression was accompanied by decreased *p16Ink4a* expression upon IOP elevation in $Six6^{+/-}$ retinas (Figures 6A and 6B). Interestingly, in $Six6^{+/-}$ mice, no β-gal-positive cells could be observed (Figures 6C and S6A), suggesting that haploinsufficiency of SIX6 was sufficiently protective against senescence in RGCs.

Together, these results suggest a model in which increased *p16Ink4a* expression is a major cause of cellular senescence in glaucoma. We then tested whether the lack of *p16Ink4a* expression in $p16Ink4a^{-/-}$ mice could prevent RGC death in our acute glaucoma model. Indeed, consistent with the above data, absence of *p16Ink4a* expression protected against RGC death (Figure 6D).

Because *P53* has been reported to play an important role in senescence (Campisi, 2013), we asked whether the lack of *P53* can prevent RGC death caused by IOP elevation. To test this, we compared the numbers of RGCs in IOP-treated mouse retinas from $p53^{-/-}$ mice to IOP-treated WT mice. We found that the lack of *p53* significantly attenuated RGC death upon IOP compared with WT mice (Figure 6E). We also observed a

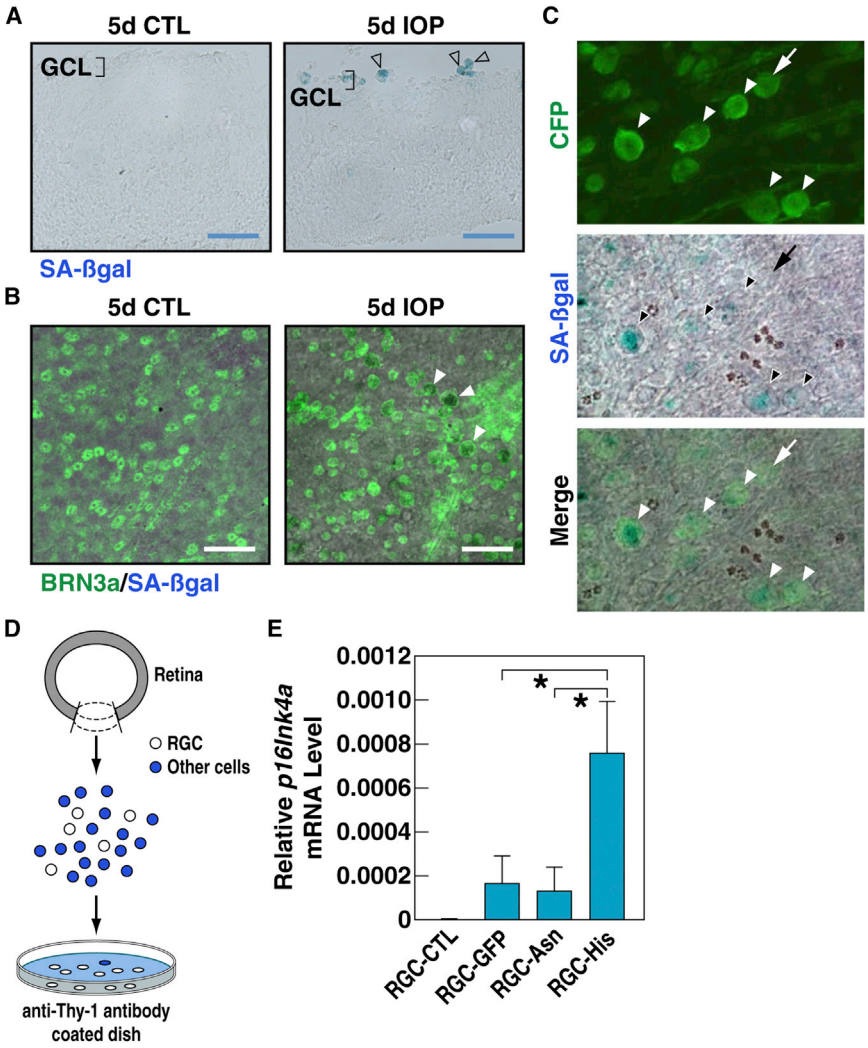

Figure 5. IOP Elevation Primarily Affects RGCs

(A) SA-βgal staining of cross-sections in IOP-treated (5d IOP) or non-treated (5d CTL) retinas. Senescent cells are localized in the GCL (blue bar, 50 μm).

(B) Double staining of IOP-treated (5d IOP) or non-treated (5d CTL) flat-mount retinas with SA-βgal and BRN3a antibodies. Most senescent cells are also BRN3a positive (arrowheads, double positive cells; white bar, 50 μm).

(C) Immunostaining of IOP-treated Thy1-CFP retinas using anti-GFP antibody. The majority of SA-βgal-positive cells are also Thy1-GFP positive (arrowheads, double positive cells; arrow, non-senescent RGC).

(D) Schematic diagram of immunopanning.

(E) His but not the Asn version of SIX6 significantly upregulates *p16Ink4a* expression compared with non-transfected (RGC-CTL) or GFP-transfected (RGC-GFP) purified rat RGCs. The p values were calculated using a two-tailed Student's t test (±SD; $^*p < 0.05$).

See also Figure S5.

genetic association of a missense variant in *P53* (rs1042522) (Genbank: NM_000546.5, c.215C > G; Genbank: NP_000537.3, p.Pro72Arg) with POAG, consistent with its role in glaucoma pathogenesis (Figure S6B).

Taken together, these findings lead us to propose a model (Figure 6F) in which IOP elevation causes the upregulation of *p16INK4a* through increased expression of SIX6 (in particular the His variant) and its binding to the *p16INK4a* promoter. Increased *p16INK4a* expression causes RGCs to enter cellular senescence. Prolonged senescence can cause increased RGC death and consequent blindness.

DISCUSSION

Glaucoma is the leading cause of blindness, affecting tens of millions of people worldwide. Despite its prevalence, its etiology and pathogenesis are poorly understood, and treatment is limited to lowering IOP. Despite aggressive IOP-lowering therapies, most patients have progressive loss of visual function, and some eventually become legally blind. The relationship of raised IOP and RGC death is poorly understood.

Cellular senescence is a state of irreversible growth arrest. When senescent cells accumulate in the tissue, their impaired function can result in a predisposition to disease development and/or progression (Baker et al., 2011; Burton, 2009; Campisi, 2013). In the present study, we show that *SIX6* directly regulates expression of *p16INK4a*, an indicator of cell senescence and aging. Furthermore, we show that upon acute IOP elevation, *p16INK4a* expression is upregulated, which, in turn, can be a cause of RGC death. Therefore *p16INK4a* upregulation appears to be a downstream integrator of diverse signals such as inherited genetic risk, age, and other factors, such as raised IOP. Our hypothesis can help explain how IOP, the most common risk factor, can cause glaucoma. Moreover, it provides a molecular link between genetic susceptibility and other factors to the pathogenesis of glaucoma.

Our study suggests that cellular senescence plays a critical role in the pathogenesis of glaucoma. Consistent with this notion, we show that another key player in cellular senescence, *P53* (Campisi, 2013), also contributes to RGC death, as evidenced by protection of RGC from IOP induced damage in mice lacking *p53*. Additionally, we provide data showing increased expression of secretory molecules, components of SASP, upon IOP-induced retinal damage. Moreover, we recently demonstrated that induction of interleukin-1 (IL1) is an early response to IOP-induced RGC damage (Chi et al., 2014). Induction of IL1, in turn, is known to cause activation of NF-kB-dependent senescence-associated expression of IL6 and interleukin-8 (Orjalo et al., 2009). Our data thus suggest that the senescence-associated cytokine network is activated in IOP-treated retinas.

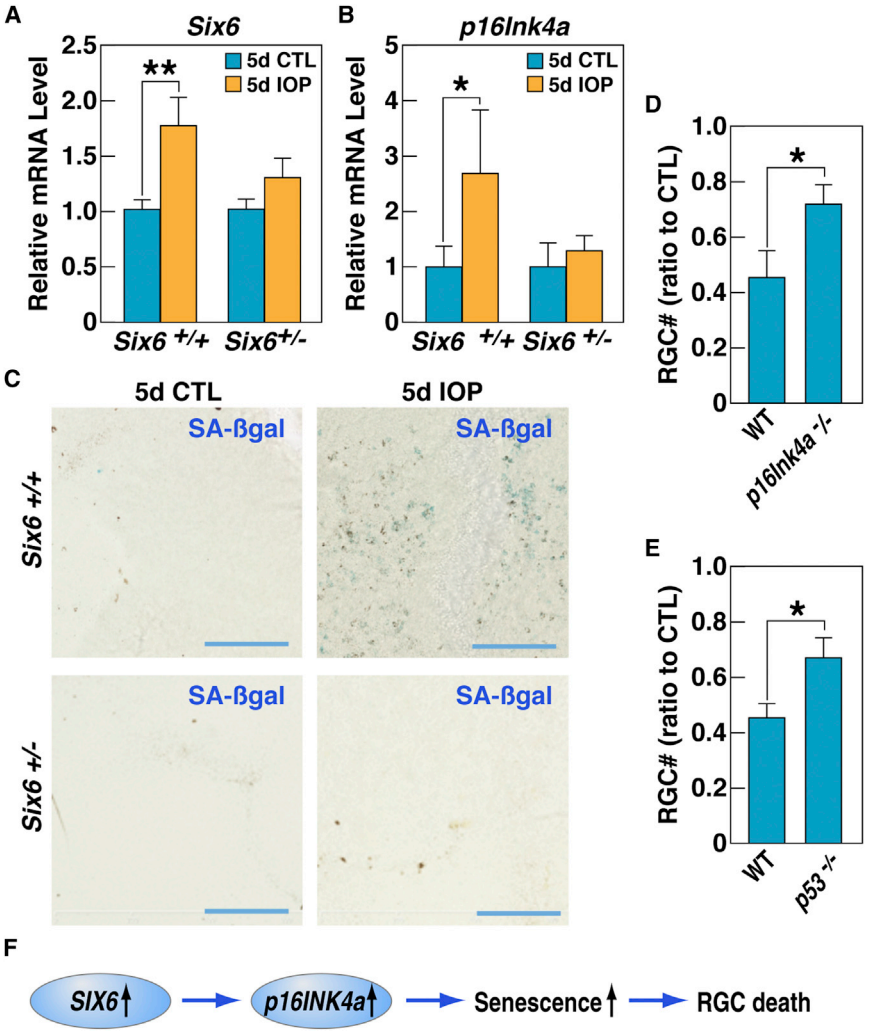

Figure 6. Absence of Either *Six6* or *p16INK4a* Protects against RGC Death in Glaucoma

(A and B) RT-qPCR analysis of *Six6* (A) and *p16Ink4a* (B) mRNA levels upon IOP treatment (5d IOP) shows elevated expression of *Six6* and *p16Ink4a* only in WT ($Six6^{+/+}$) retinas and not in $Six6^{+/-}$ retinas compared with non-treated (5d CTL) retinas. Experiments repeated in eight animals; p values were calculated using a two-tailed Student's t test (±SD; *$p < 0.05$, **$p < 0.01$).

(C) SA-βgal staining of flat-mount retinas isolated from IOP-treated and non-treated eyes of $Six6^{+/+}$ and $Six6^{+/-}$ mice shows a lack of senescent cells in the treated tissue isolated from heterozygous mice (blue bar, 100 μm).

(D) Quantification of the RGC ratio in treated and non-treated retinas in WT and $p16Ink4a^{-/-}$ mice.

(E) Quantification of the RGC ratio in IOP-treated and non-treated retinas in WT and *p53* KO mice.

(F) Model of the sequence of events leading to RGC death upon Six6 upregulation in glaucoma.

See also Figure S6.

p16INK4a is a cyclin-dependent kinase inhibitor and a potent negative regulator of cell-cycle progression. Consequently, upregulated *p16INK4a* expression and senescence phenotype, as measured by SA-βgal assay and SASP, usually indicate the irreversible cell-cycle arrest (Campisi, 2013). In our study, however, elevated *p16INK4a* expression and senescence were observed in RGCs (post-mitotic neurons), which are believed not to be replication competent. Therefore, one possibility is that RGCs may contain a replication-competent, stem cell-like population; alternatively, *p16INK4a* may play a previously unrecognized role in these post-mitotic cells.

Although the primary focus of the present study was on the role of *p16INK4a* on RGC death, our data do not exclude a potential role for other genes located in the 9p21 locus in the pathology of glaucoma. For example, *p14ARF* may contribute to glaucoma pathogenesis independently by influencing eye vasculature development (McKeller et al., 2002). Further studies are required to elucidate role of *p14ARF* and p15CDKN2B in the pathogenesis of glaucoma.

SIX6 is a member of the SIX/Sine oculis family of homeobox transcription factors involved in the development of retina (Gallardo et al., 1999; López-Ríos et al., 1999). It has been shown to directly regulate the expression of cyclin-dependent kinase inhibitor genes (Li et al., 2002) as well as GnRH (Larder et al., 2011) during mouse development. Although the role of *SIX6* during retina development is being investigated by a number of laboratories, there are very few reports exploring its molecular role in adult retina or in glaucoma pathogenesis. Several *SIX6* mutations and SNPs have been shown to correlate with developmental eye defects in human (Aldahmesh et al., 2013; Gallardo et al., 1999, 2004). Additionally, several SNPs have been associated with an increased risk for glaucoma (Carnes et al., 2014; Iglesias et al., 2014). The effects of *SIX6* variants had always been assessed after late identification of the disease, and this approach does not allow for correct dissociation of developmental defects from the genetic components that cause the disease.

The *SIX6* variant referred to as "risk" (histidine-encoding SIX6-His) is actually evolutionary conserved across the phyla. The Asn variant (the protective allele for glaucoma) is detected only in the human branch; however, it is unknown why it would be advantageous for humans to have a protective variant. Several groups performed rescue experiments by overexpressing human His variant in zebrafish and found that it did not rescue eye defects induced by the removal of endogenous SIX6 proteins. Interestingly, both *zSix6a* and *zSix6b* carry the His amino acid at the orthologous position (Carnes et al., 2014; Iglesias et al., 2014). These results suggest that the inability to rescue eye phenotypes by human His version of SIX6 is likely the result of species-specific differences in other residues and not the sole effect of His/Asn variant.

Taken together, our study shows that SIX6 His variant increases *p16INK4a* expression upon increased IOP, which in turn causes RGCs to enter into a senescent state and which may lead to increased RGC death in glaucoma. Our study provides important insights into the pathogenesis of glaucoma and suggests future therapeutic strategies based on targeted inhibition of *p16INK4a*-induced cell senescence to prevent and treat glaucoma.

EXPERIMENTAL PROCEDURES

Subjects and Test Procedure

This study was approved by the institutional review boards (IRBs) of the University of California, San Diego, the University of Southern California, and West China Hospital. All participants signed informed-consent statements prior to participation. Blood was drawn from a vein in the patient's arm into blood collection tubes containing the anticoagulant acid citrate dextrose. Genomic DNA was extracted from peripheral blood leukocytes with the Qiagen kit, according to the manufacturer's instructions. For the initial cohort, 1,130 POAG patients and 4,036 controls were enrolled in this study. All participants were of European descent. For the Mexican cohort, 105 POAG patients and 188 controls were enrolled in this study.

Clinical Definitions

Clinical assessment was performed using previously described methods (Wiggs et al., 2012). POAG patients were defined as individuals for whom reliable visual field (VF) tests showed characteristic VF defects consistent with glaucomatous optic neuropathy. Individuals were classified as affected if the VF defects were reproduced on a subsequent test or if a single qualifying VF was accompanied by a cup-disc ratio (CDR) of 0.7 or more in at least one eye. The examination of the ocular anterior segment did not show signs of secondary causes for elevated IOP, such as exfoliation syndrome or pigment dispersion syndrome, and the filtration structures were deemed to be open on the basis of clinical measures. Controls had normal optic nerves (CDRs $\leq$ 0.6) and normal IOP (Wiggs et al., 2012).

Genotyping and Statistical Analysis

Genomic DNA was extracted from peripheral blood leukocytes with the Qiagen kit, according to the manufacturer's instructions. rs33912345 (C/A) in *SIX6,* rs3731239 (A/G) in *p16INK4a*, and rs1042522 (C/G) in *P53* were genotyped using single-nucleotide primer extension assay (ABI Prism SNaPShot Multiplex Kit; Applied Biosystems) on an ABI 3130xl genetic analyzer, as previously described (Yang et al., 2006). The primers used for genotyping are listed in Table S2. SNP genotyping results were screened for deviation from Hardy-Weinberg equilibrium using chi-square tests. Allele association was calculated with a chi-square test performed using the program PLINK (Purcell et al., 2007) (RRID: nlx_154200; http://pngu.mgh.harvard.edu/purcell/plink/). Asymptomatic p values were also generated for this test.

Joint Effects of *SIX6*-rs33912345 and *p16INK4a*-rs3731239

Joint effects of *SIX*6-rs33912345 (C/A) and *p16INK4a*-rs3731239 (A/G) were calculated by a logistic regression model (Chen et al., 2010, 2011). A global two-locus (9′2) contingency table, enumerating all nine two-locus genotype combinations, was constructed. ORs and 95% CIs, comparing each genotypic combination with the baseline of homozygosity for the common allele at both loci, were calculated, according to the previously described methods (Chen et al., 2010, 2011).

Three-Dimensional Modeling of the SIX6 H141N Variation

We performed a computer modeling analysis to investigate the effects of the *SIX6* His141Asn variation on the 3D structure and function of SIX6 with the ICM software (Cardozo et al., 1995). The SIX6 transcription factor has never been crystallized for X-ray analysis or studied by nuclear magnetic resonance (NMR). To build a structural model of the DNA-binding domain around the H141N variation, we searched the Protein Data Bank for homologous transcription factors. The search identified the following entries with fragments of related transcription factors: 2DMU, 1QRY, 1VND, 1YRN, 2LKX, and two solved by crystallography or NMR. Then we attempted a structural superposition of the identified domains. All had a structurally (topologically) similar DNA-binding motif, covering the area from residues around 134–189. The structural homology model of SIX6 was built for residues from 134–189 with the ICM software (Cardozo et al., 1995) by threading the SIX6 sequence onto the consensus structure.

Lymphoblastoid Cell Lines Culture

The human lymphoblastoid cell lines were generated by the method "General Protocol for the Immortalization of Human B-Lymphocytes Using EBV" (http://www.unclineberger.org/tissueculture/protocols/b-lymphocytesprotocol). Four lymphoblastoid cell lines with the genotypes of *SIX6* rs33912345-CC and another four with the genotypes of *SIX6* rs33912345-AA were used. The cells were cultured in RPMI-1640 base medium (61870127; Invitrogen) supplemented with 20% fetal bovine serum and 1 × penicillin-streptomycin (P0781; Sigma). RNA was extracted and the total mRNA levels of *SIX6* and *p16INK4a* were measured by RT-qPCR.

Acute IOP Mouse Model

Unilateral elevation of IOP in 1-month-old C57BL/6J, *p16Ink4a*$^{-/-}$, Thy1-CFP (Lindsey et al., 2013), *Six6*$^{+/-}$ (Larder et al., 2011), and *p53*$^{-/-}$ (129-Trp53tm1Tyj/J; The Jackson Laboratory) mice was achieved through instilling the anterior chamber with saline solution and maintained at an elevated pressure of 90 mm Hg. The *p16Ink4a*$^{-/-}$ line was engineered to remove the common exon of E2 and E3; therefore, the line is a null allele for both *p16Ink4a* and *p19Arf* genes (Serrano et al., 1996). IOP was measured by a tonometer. All procedures were conducted with the approval and under the supervision of the Institutional Animal Care Committee at the University of California, San Diego, and adherence to the ARVO Statement for the Use of Animals in Ophthalmic and Vision Research. C57BL/6J male mice were purchased from The Jackson Laboratory. To elevate IOP experimentally, animals were first anesthetized with a weight-based intraperitoneal injection of ketamine (80 mg/kg) and xylazine (16 mg/kg). Additional anesthesia was provided via the same route at 45 min intervals. Corneal anesthesia was achieved with a single drop of 0.5% proparacaine hydrochloride (Alcon Laboratories). A drop of 0.5% proparacaine hydrochloride and 0.5% tropicamide (Alcon Laboratories) was then applied to the right eye. Body temperature was maintained between 37°C and 38°C, with a water-heat pad (TP500T/Pump; Gaymar Industries). A 30-gauge needle was used to puncture the mid-peripheral cornea of the right eye; the anterior chambers were cannulated with sterile physiologic saline (balanced salt solution; Alcon Laboratories), and IOP was manometrically controlled by adjusting the saline height. IOP was monitored with an indentation tonometer (Tonolab; Icare) and maintained at 90 mm Hg pressure for 1 hr. Assessment of the senescence of RGCs was made in retinal flat mounts harvested 5 days after experiments. In brief, mice were euthanized with CO_2, and eyeballs were dissected and fixed in ice-cold phosphate-buffered 4% paraformaldehyde (pH 7.4) for 30 min, followed by flat mounting of the retinas.

SA-βgal Assay to Test Senescence on Retinas from Human and IOP Mouse Eyes

Senescence assays were performed using the Senescence β-Galactosidase Staining Kit (Cell Signaling) according to the manufacturer's protocol. For double staining, senescence assays were followed by anti-GFP antibody staining to reveal full fluorescence of Thy1-CFP retinas.

RNA Extraction and Real-Time PCR

Total RNA extraction from mouse tissues or human lymphoblastoid cells, cDNA synthesis, and RT-qPCR experiments were performed as previously described (Luo et al., 2013). Assays were performed in triplicate. Relative mRNA levels were calculated by normalizing results using *GAPDH*. The primers used for RT-qPCR are listed in Table S2. The differences in quantitative PCR data were analyzed with an independent two-sample t test.

Human fRPC Isolation and Expansion

All work with human material was performed with IRB approval. fRPCs were isolated from human fetal neural retina at 16 weeks gestational age, as

previously described (Luo et al., 2014). Whole neuroretina was separated from the retinal pigment epithelium layer, minced, and digested with collagenase I (Sigma-Aldrich). Cells and cell clusters were plated onto human fibronectin (Akron)-coated flasks (Nunclon Delta) in Ultraculture Media (Lonza), supplemented with 2 mM L-glutamine (Invitrogen), 10 ng/ml rhbFGF (Peprotech), and 20 ng/ml rhEGF (Peprotech) in a low-oxygen incubator (37°C, 3% O_2, 5% CO_2, 100% humidity). Cells were passaged at 80% confluency using TrypZean (Sigma-Aldrich), benzonase (EMD Chemicals), and Defined Trypsin Inhibitor (Invitrogen).

Immunopanning

The immunopanning procedure and RGC culture were performed according to the published detailed protocol (Winzeler and Wang, 2013).

Plasmid Transfection into Human Embryonic Kidney 293 Cells and fRPCs

Overexpression was performed using Lipofectamine 2000 (Invitrogen) according to the manufacturer's standard protocol. Empty or GFP-containing vector was used as a negative control. For ChIP and expression analysis experiments, cells were harvested 48 hr post-transfection. For senescence analysis in fRPCs, cells were collected after 24 hr.

ChIP

ChIP was performed as previously described (Skowronska-Krawczyk et al., 2004, 2009). Briefly, cells or dissected retinas were fixed for 10 min with 1% formaldehyde; chromatin was isolated and sonicated to obtain fragments 300–700 bp in length. After adding antibodies, immunoprecipitation was carried out overnight, and protein/DNA complexes were pulled out using protein G-coated magnetic beads (Invitrogen). After 3 washes, DNA crosslinking was reversed. The DNA was then purified and subjected to qPCR. All experiments were repeated at least three times. The p values were calculated using Student's t tests.

Antibodies

Antibodies used in this study included guinea pig anti-SIX6 (a generous gift from Dr. Xue Li's lab), rabbit anti-SIX6 (Abcam, cat# ab64995, RRID: AB_1140739), anti-H3Ac (Millipore, cat# 06-599, RRID: AB_2115283), anti-HA (1867431; Roche), anti-p-300 (C-20; Santa Cruz), anti-BRN3a (Millipore, cat# MAB1585, RRID: AB_94166), anti-GFP (Aves Labs, cat# GFP-1020, RRID: AB_10000240), and anti-IL6 (Abcam, cat# ab83339, RRID: AB_10561794).

SUPPLEMENTAL INFORMATION

Supplemental Information includes six figures and two tables and can be found with this article online at http://dx.doi.org/10.1016/j.molcel.2015.07.027.

AUTHOR CONTRIBUTIONS

K.Z., D.S.-K., Y.L., and L.Z. designed the study. D.S.-K., L.Z., J.Z., R.N.W., J.L., K.F., S.P., C.W., M.K., H.L., H.O., D.L., W.W., G.L., Y.X., G.C., O.L., C.C., E.Y., M.J., M.A., Z.Z., W.S., L.Z., M.K., D.C., C.S., C.Z., J.Z., P.L.M., W.G., L.Z., X.S., S.Z., Y.Z., M.G.R., Y.L., and K.Z. performed experiments, provided reagents and patient cohorts, and analyzed results. K.Z., D.S.-K., L.Z., and R.N.W. wrote the manuscript.

ACKNOWLEDGMENTS

This study was supported in part by the 973 Program (2015CB94600 and 2013CB967504), the State Key Laboratory of Ophthalmology, and NIH grants RO1HG008135, R01EY023704, R01 HD072754, and P30EY022589, Research to Prevent Blindness. We thank J. Hightower for figure preparation. D.S.-K. was supported by a European Molecular Biology Organization Long-Term Fellowship, the Swiss National Science Foundation, and the San Diego Foundation.

Received: February 19, 2015
Revised: June 8, 2015
Accepted: July 24, 2015
Published: September 10, 2015

REFERENCES

Aldahmesh, M.A., Khan, A.O., Hijazi, H., and Alkuraya, F.S. (2013). Homozygous truncation of SIX6 causes complex microphthalmia in humans. Clin. Genet. *84*, 198–199.

Anderson, A.M., Weasner, B.M., Weasner, B.P., and Kumar, J.P. (2012). Dual transcriptional activities of SIX proteins define their roles in normal and ectopic eye development. Development *139*, 991–1000.

Baker, D.J., Wijshake, T., Tchkonia, T., LeBrasseur, N.K., Childs, B.G., van de Sluis, B., Kirkland, J.L., and van Deursen, J.M. (2011). Clearance of p16Ink4a-positive senescent cells delays ageing-associated disorders. Nature *479*, 232–236.

Burdon, K.P., Macgregor, S., Hewitt, A.W., Sharma, S., Chidlow, G., Mills, R.A., Danoy, P., Casson, R., Viswanathan, A.C., Liu, J.Z., et al. (2011). Genome-wide association study identifies susceptibility loci for open angle glaucoma at TMCO1 and CDKN2B-AS1. Nat. Genet. *43*, 574–578.

Burton, D.G. (2009). Cellular senescence, ageing and disease. Age (Dordr.) *31*, 1–9.

Campisi, J. (2013). Aging, cellular senescence, and cancer. Annu. Rev. Physiol. *75*, 685–705.

Cardozo, T., Totrov, M., and Abagyan, R. (1995). Homology modeling by the ICM method. Proteins *23*, 403–414.

Carnes, M.U., Liu, Y.P., Allingham, R.R., Whigham, B.T., Havens, S., Garrett, M.E., Qiao, C., Katsanis, N., Wiggs, J.L., Pasquale, L.R., et al.; NEIGHBORHOOD Consortium Investigators (2014). Discovery and functional annotation of SIX6 variants in primary open-angle glaucoma. PLoS Genet. *10*, e1004372.

Chen, Y., Bedell, M., and Zhang, K. (2010). Age-related macular degeneration: genetic and environmental factors of disease. Mol. Interv. *10*, 271–281.

Chen, Y., Zeng, J., Zhao, C., Wang, K., Trood, E., Buehler, J., Weed, M., Kasuga, D., Bernstein, P.S., Hughes, G., et al. (2011). Assessing susceptibility to age-related macular degeneration with genetic markers and environmental factors. Arch. Ophthalmol. *129*, 344–351.

Chi, W., Li, F., Chen, H., Wang, Y., Zhu, Y., Yang, X., Zhu, J., Wu, F., Ouyang, H., Ge, J., et al. (2014). Caspase-8 promotes NLRP1/NLRP3 inflammasome activation and IL-1β production in acute glaucoma. Proc. Natl. Acad. Sci. U S A *111*, 11181–11186.

Clark, D.D., Gorman, M.R., Hatori, M., Meadows, J.D., Panda, S., and Mellon, P.L. (2013). Aberrant development of the suprachiasmatic nucleus and circadian rhythms in mice lacking the homeodomain protein Six6. J. Biol. Rhythms *28*, 15–25.

Gallardo, M.E., Lopez-Rios, J., Fernaud-Espinosa, I., Granadino, B., Sanz, R., Ramos, C., Ayuso, C., Seller, M.J., Brunner, H.G., Bovolenta, P., and Rodríguez de Córdoba, S. (1999). Genomic cloning and characterization of the human homeobox gene SIX6 reveals a cluster of SIX genes in chromosome 14 and associates SIX6 hemizygosity with bilateral anophthalmia and pituitary anomalies. Genomics *61*, 82–91.

Gallardo, M.E., Rodríguez De Córdoba, S., Schneider, A.S., Dwyer, M.A., Ayuso, C., and Bovolenta, P. (2004). Analysis of the developmental SIX6 homeobox gene in patients with anophthalmia/microphthalmia. Am. J. Med. Genet. A *129A*, 92–94.

Gross, R.L., Ji, J., Chang, P., Pennesi, M.E., Yang, Z., Zhang, J., and Wu, S.M. (2003). A mouse model of elevated intraocular pressure: retina and optic nerve findings. Trans. Am. Ophthalmol. Soc. *101*, 163–169, discussion 169–171.

Iglesias, A.I., Springelkamp, H., van der Linde, H., Severijnen, L.A., Amin, N., Oostra, B., Kockx, C.E., van den Hout, M.C., van Ijcken, W.F., Hofman, A., et al. (2014). Exome sequencing and functional analyses suggest that SIX6 is a gene involved in an altered proliferation-differentiation balance early in life and optic nerve degeneration at old age. Hum. Mol. Genet. *23*, 1320–1332.

Krishnamurthy, J., Torrice, C., Ramsey, M.R., Kovalev, G.I., Al-Regaiey, K., Su, L., and Sharpless, N.E. (2004). Ink4a/Arf expression is a biomarker of aging. J. Clin. Invest. *114*, 1299–1307.

Larder, R., Clark, D.D., Miller, N.L., and Mellon, P.L. (2011). Hypothalamic dysregulation and infertility in mice lacking the homeodomain protein Six6. J. Neurosci. *31*, 426–438.

Li, X., Perissi, V., Liu, F., Rose, D.W., and Rosenfeld, M.G. (2002). Tissue-specific regulation of retinal and pituitary precursor cell proliferation. Science *297*, 1180–1183.

Lindsey, J.D., Duong-Polk, K.X., Dai, Y., Nguyen, D.H., Leung, C.K., and Weinreb, R.N. (2013). Protection by an oral disubstituted hydroxylamine derivative against loss of retinal ganglion cell differentiation following optic nerve crush. PLoS ONE *8*, e65966.

López-Ríos, J., Gallardo, M.E., Rodriguez de Córdoba, S., and Bovolenta, P. (1999). Six9 (Optx2), a new member of the six gene family of transcription factors, is expressed at early stages of vertebrate ocular and pituitary development. Mech. Dev. *83*, 155–159.

Luo, J., Zhao, L., Chen, A.Y., Zhang, X., Zhu, J., Zhao, J., Ouyang, H., Luo, H., Song, Y., Lee, J., et al. (2013). TCF7L2 variation and proliferative diabetic retinopathy. Diabetes *62*, 2613–2617.

Luo, J., Baranov, P., Patel, S., Ouyang, H., Quach, J., Wu, F., Qiu, A., Luo, H., Hicks, C., Zeng, J., et al. (2014). Human retinal progenitor cell transplantation preserves vision. J. Biol. Chem. *289*, 6362–6371.

McKeller, R.N., Fowler, J.L., Cunningham, J.J., Warner, N., Smeyne, R.J., Zindy, F., and Skapek, S.X. (2002). The Arf tumor suppressor gene promotes hyaloid vascular regression during mouse eye development. Proc. Natl. Acad. Sci. U S A *99*, 3848–3853.

Naylor, R.M., Baker, D.J., and van Deursen, J.M. (2013). Senescent cells: a novel therapeutic target for aging and age-related diseases. Clin. Pharmacol. Ther. *93*, 105–116.

Orjalo, A.V., Bhaumik, D., Gengler, B.K., Scott, G.K., and Campisi, J. (2009). Cell surface-bound IL-1alpha is an upstream regulator of the senescence-associated IL-6/IL-8 cytokine network. Proc. Natl. Acad. Sci. U S A *106*, 17031–17036.

Osman, W., Low, S.K., Takahashi, A., Kubo, M., and Nakamura, Y. (2012). A genome-wide association study in the Japanese population confirms 9p21 and 14q23 as susceptibility loci for primary open angle glaucoma. Hum. Mol. Genet. *21*, 2836–2842.

Purcell, S., Neale, B., Todd-Brown, K., Thomas, L., Ferreira, M.A.R., Bender, D., Maller, J., Sklar, P., de Bakker, P.I.W., Daly, M.J., and Sham, P.C. (2007). PLINK: a toolset for whole-genome association and population-based linkage analysis. Am. J. Hum. Genet. *81*, 559–575.

Serrano, M., Lee, H., Chin, L., Cordon-Cardo, C., Beach, D., and DePinho, R.A. (1996). Role of the INK4a locus in tumor suppression and cell mortality. Cell *85*, 27–37.

Skowronska-Krawczyk, D., Ballivet, M., Dynlacht, B.D., and Matter, J.M. (2004). Highly specific interactions between bHLH transcription factors and chromatin during retina development. Development *131*, 4447–4454.

Skowronska-Krawczyk, D., Chiodini, F., Ebeling, M., Alliod, C., Kundzewicz, A., Castro, D., Ballivet, M., Guillemot, F., Matter-Sadzinski, L., and Matter, J.M. (2009). Conserved regulatory sequences in Atoh7 mediate non-conserved regulatory responses in retina ontogenesis. Development *136*, 3767–3777.

Strahl, B.D., and Allis, C.D. (2000). The language of covalent histone modifications. Nature *403*, 41–45.

Wang, X., Pan, L., Feng, Y., Wang, Y., Han, Q., Han, L., Han, S., Guo, J., Huang, B., and Lu, J. (2008). P300 plays a role in p16(INK4a) expression and cell cycle arrest. Oncogene *27*, 1894–1904.

Weinreb, R.N., Aung, T., and Medeiros, F.A. (2014). The pathophysiology and treatment of glaucoma. JAMA *311*, 1901–1911.

Wiggs, J.L., Yaspan, B.L., Hauser, M.A., Kang, J.H., Allingham, R.R., Olson, L.M., Abdrabou, W., Fan, B.J., Wang, D.Y., Brodeur, W., et al. (2012). Common variants at 9p21 and 8q22 are associated with increased susceptibility to optic nerve degeneration in glaucoma. PLoS Genet. *8*, e1002654.

Winzeler, A., and Wang, J.T. (2013). Purification and culture of retinal ganglion cells from rodents. Cold Spring Harb. Protoc. *2013*, 643–652.

Yang, Z., Camp, N.J., Sun, H., Tong, Z., Gibbs, D., Cameron, D.J., Chen, H., Zhao, Y., Pearson, E., Li, X., et al. (2006). A variant of the HTRA1 gene increases susceptibility to age-related macular degeneration. Science *314*, 992–993.

Zhang, K., Zhang, L., and Weinreb, R.N. (2012). Ophthalmic drug discovery: novel targets and mechanisms for retinal diseases and glaucoma. Nat. Rev. Drug Discov. *11*, 541–559.